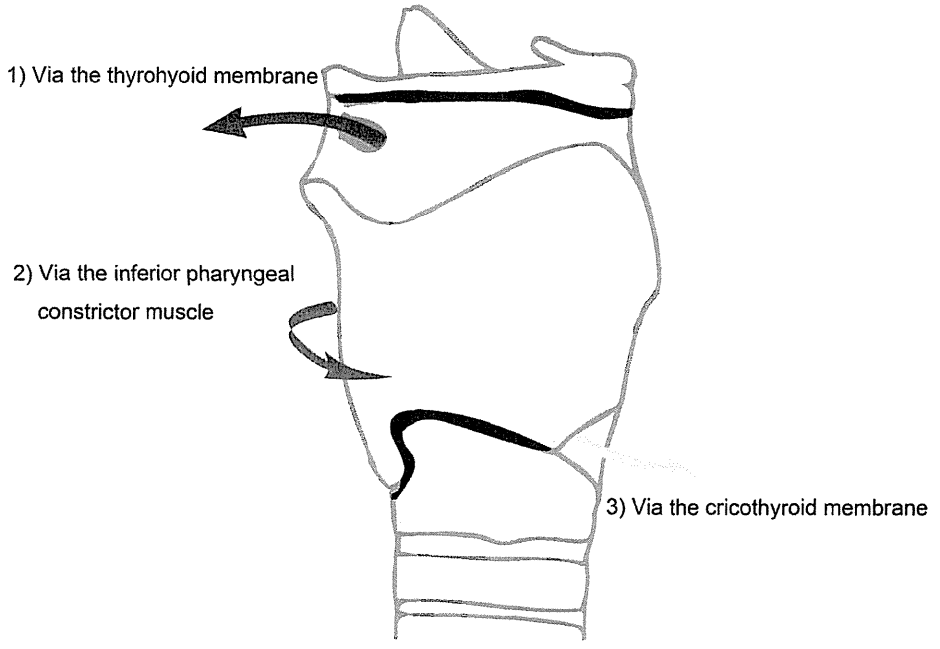

Fig. 11. Drawings (right lateral view of laryngeal box) illustrate the routes of tumor spread out from the larynx through areas of inherent weakness; (1) via the thyrohyoid membrane along the superior laryngeal neurovascular bundle (red arrow), (2) via the inferior pharyngeal constrictor muscle (blue arrow), (3) via the cricothyroid membrane (yellow arrow).

esophagus, trachea, or deep lingual muscle, with or without cartilage penetration [20]. In clinical practice, patients with T4 disease do not always inevitably undergo laryngectomy, and for patients without tumor extension through the cartilage – a diagnosis that is not always straightforward – clinicians rely on imaging for accurate tumor staging, tumor mapping and detection of possible tumor extension [5,6]. It is then possible to predict which patients may be candidates for function-preserving treatments to some degree, and discussions with the patients are part of the treatment decision process.

According to Beitler et al. [39], extralaryngeal spread without thyroid cartilage penetration was more common than previously expected in patients with advanced laryngeal and hypopharyngeal cancer. The authors suggested that cartilage invasion was absent in 40% of cases showing extralaryngeal tumor spread. Since extralaryngeal tumor spread is one of the important predictors of T4 disease in laryngeal and hypopharyngeal cancer, the focus of imaging needs to shift from detection of invasion to reliably demonstrating more extensive disease.

4.2.1. Conventional CT

Extralaryngeal spread can be considered if the following features can be identified: substitution by tumor tissue on the outside of the membrane/cartilage, or loss of fat attenuation between the extralaryngeal structure (such as blood vessel or muscle) and laryngeal components. To detect extralaryngeal spread, it is important to thoroughly understand the complex anatomy in this area and the imaging features of commonly occurring extension patterns (Fig. 11). One of the most common routes of lesion spread from the larynx through areas of inherent weakness is via the thyrohyoid membrane (Fig. 12). The superior laryngeal neurovascular bundle enters the laryngeal component through a posterolateral defect in the thyrohyoid membrane; this defect is known to be the route by which tumors spread [48,49]. Another route of extralaryngeal spread, especially in the case of piriform sinus cancer, is via the inferior pharyngeal constrictor muscle [48,50] on the basis of its attachment to the lamina of the thyroid cartilage (Fig. 13). Sometimes, the tumor may show submucosal extension to the extralaryngeal soft tissue via the cricothyroid membrane (Fig. 14). Such extension into deep-seated tissue planes is difficult to evaluate by clinical inspection examination alone.

4.2.2. MR imaging

Diagnosis of extralaryngeal spread on the basis of MR imaging is based mainly on altered signal behavior of extralaryngeal soft tissue with different pulse sequences. Extralaryngeal spread is considered to be present when signals in the fat component of extralaryngeal soft tissue continuous with the primary tumor have an intensity similar to that of the tumor on T2WI, are hypointense on T1WI, and hyperintense on contrast-enhanced T1WI.

4.2.3. Dual-energy CT

Extralaryngeal spread can be identified on CT or MR imaging, but dual-energy CT may facilitate a clearer diagnosis. The IO images generated by using dual-energy CT reveal the area of tumor spread into soft tissue as red-colored enhancement, because IO images visualize areas of iodine distribution in soft tissue (Figs. 12B, 13B and 14C). The preliminarily reported sensitivity and specificity of WA plus IO images for extralaryngeal spread are 100% (14/14) and 100% (16/16), respectively [16]. Regardless of whether cartilage invasion is present, combined analysis of WA and IO images may also be useful for evaluating extralaryngeal spread of advanced laryngeal and hypopharyngeal cancer.

5. A diagnostic algorithm including dual-energy CT

All patients with symptoms that are suggestive of laryngeal or hypopharyngeal cancer should undergo a thorough assessment

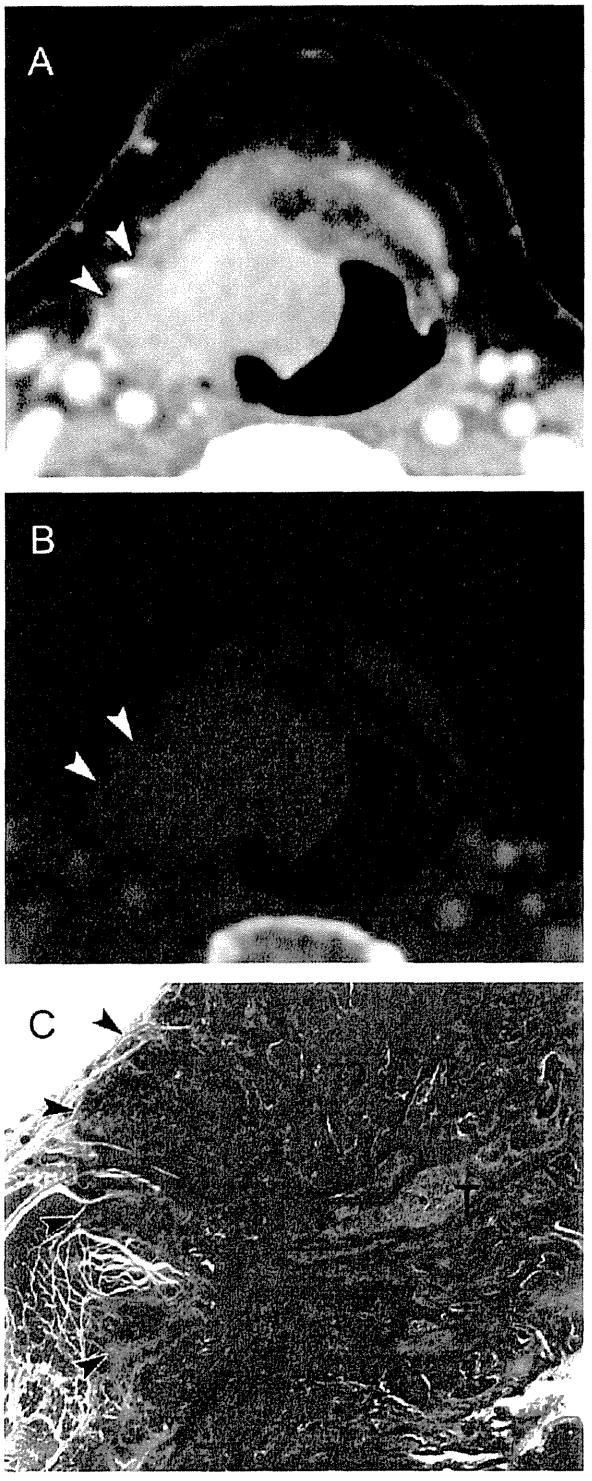

Fig. 12. Extralaryngeal spread via the thyrohyoid membrane on dual-energy CT in a 78-year-old man with supraglottic cancer. (A) WA image shows that the tumor has invaded the right aryepiglottic fold and preepiglottic space at the superior margin of the thyroid cartilage. The tumor extends through the thyrohyoid membrane into the extralaryngeal tissues (arrowheads). (B) The IO image reveals extralaryngeal tumor spread more clearly through the thyrohyoid membrane along the superior neurovascular bundle as a red-colored area (arrowheads). (C) Microscopic analysis confirmed the infiltration of the tumor cells into the extralaryngeal soft tissue and thyrohyoid muscle (hematoxylin–eosin stain; original magnification, 5×).

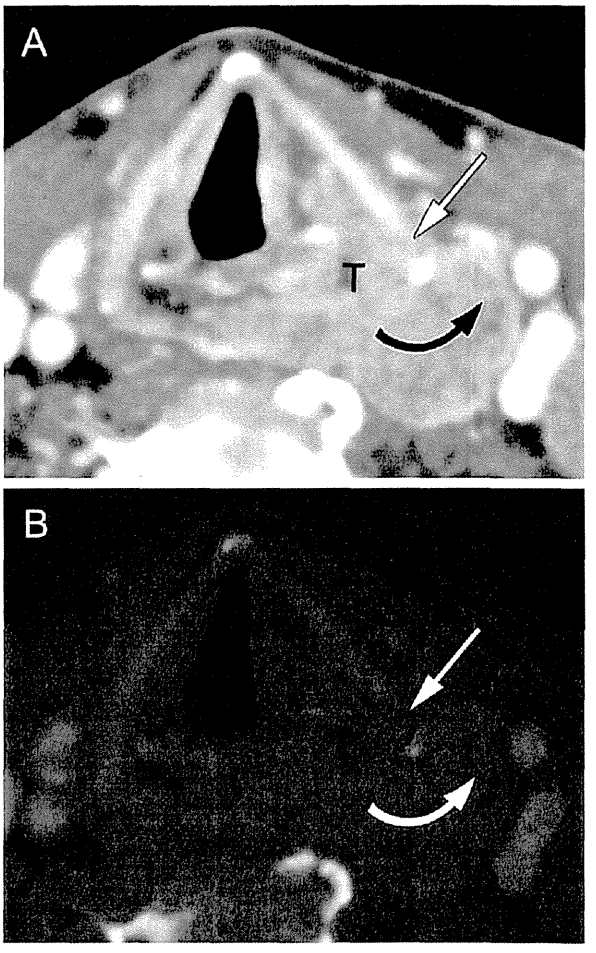

Fig. 13. Extralaryngeal spread via the inferior pharyngeal constrictor muscle on dual-energy CT in a 60-year-old man with hypopharyngeal cancer. WA image (A) and IO image (B) at the glottic level show a tumor mass (T) arising from the left piriform sinus, spreading into the lateral extralaryngeal soft tissue via the attachment of the inferior pharyngeal constrictor muscle (curved arrow). The tumor also wraps around the posterior border of the thyroid cartilage. On the WA image (A), the inner cortex of the left thyroid cartilage shows focal lysis (arrow). However, the IO image (B) shows no corresponding enhancement in the region indicated in the WA image (arrow). This case was evaluated as T4a disease without cartilage invasion and treated by chemoradiotherapy.

of their clinical history and a physical examination including nasopharyngoscopy, followed by multimodality imaging. We believe that dual-energy CT has the potential to become the primary diagnostic tool for laryngeal and hypopharyngeal cancer, although further investigation of dual-energy CT in comparison with MR will be necessary. Dual-energy CT may be very helpful for staging, including the definition of T stage, particularly when distinguishing T4 from lower-stage lesions, and for detection of regional lymph nodes (N staging) and distant metastasis (M staging). If evaluations conducted using dual-energy CT alone are insufficient, contrast-enhanced MR imaging is useful for excluding cartilage invasion, and for evaluation of very advanced local disease such as tumor invasion to the prevertebral fascia or carotid artery.

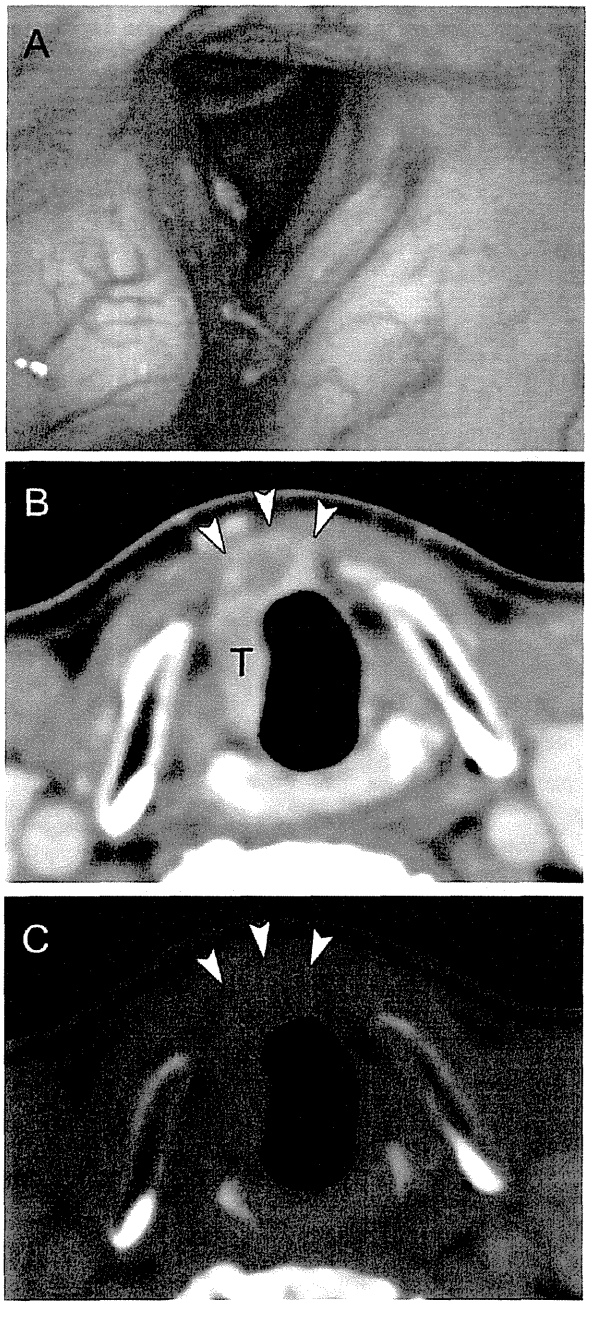

Fig. 14. Extralaryngeal spread via the cricothyroid membrane on dual-energy CT in a 72-year-old man with right glottic cancer. (A) Nasopharyngolaryngoscopy demonstrates the tumor mass (T) at the right glottis. It is diagnosed clinically as T3. WA image (B) and IO image (C) at the subglottic level show that the tumor has spread submucosally into the extralaryngeal soft tissue (arrowheads) via the cricothyroid membrane, and is therefore diagnosed as T4a.

6. Conclusion

Imaging plays a significant role in the staging of laryngeal and hypopharyngeal cancer, particularly when distinguishing the absence or presence of laryngeal cartilage invasion by the tumor and extralaryngeal spread. With conventional CT, although cartilage invasion can be diagnosed with acceptable accuracy by applying defined criteria for combinations of erosion, lysis and transmural extralaryngeal spread, iodine-enhanced tumors and non-ossified cartilage are sometimes difficult to distinguish. MR offers high contrast resolution for images without motion artifacts, although inflammatory changes in cartilage sometimes resemble cartilage invasion. With dual-energy CT, combined iodine-overlay images and weighted-average images can be used for evaluation of cartilage invasion, since iodine enhancement is evident in tumor tissue but not in cartilage. Extralaryngeal spread can be evaluated from CT, MR or dual-energy CT images and the three common routes of tumor spread into the extralaryngeal soft tissue must be considered. The ability to obtain weighted-average images and iodine-overlay images gives dual-energy CT potential advantages over conventional CT for evaluation of laryngeal and hypopharyngeal cancer. The benefit of the dual-energy technique lies in the impact of its high-quality images on treatment decision-making. Further advances in dual-energy CT may lead to its more widespread use for imaging of laryngeal and hypopharyngeal cancer. To define the most appropriate treatment strategies, it is important to thoroughly understand the potential applications, limitations, and advantages of existing and evolving imaging technologies, including dual-energy CT.

Conflict of interest

One of the authors (K.O.) is an employee of Siemens Japan. Authors who are not employees of Siemens Japan monitored and had control of inclusion of any data and information submitted for publication. No potential conflicts of interest were disclosed.

Acknowledgement

This work was supported in part by a National Cancer Center Research and Development Fund (23-A-35).

References

[1] Barnes L, Eveson JW, Riechart P, et al. 8edrs pathology and genetics of head and neck tumours. World Health Organization Classification of Tumours. Lyon: IARC; 2005. p. 107–62.
[2] Pfister DG, Laurie SA, Weinstein GS, et al. American Society of Clinical Oncology clinical practice guideline for the use of larynx-preservation strategies in the treatment of laryngeal cancer. J Clin Oncol 2006;24(22):3693–704.
[3] Hoffman HT, Porter K, Karnell LH, et al. Laryngeal cancer in the United States: changes in demographics, patterns of care, and survival. Laryngoscope 2006;116(9 Pt 2 Suppl 111):1–13.
[4] Forastiere AA, Goepfert H, Maor M, et al. Concurrent chemotherapy and radiotherapy for organ preservation in advanced laryngeal cancer. N Engl J Med 2003;349(22):2091–8.
[5] Knab BR, Salama JK, Solanki A, et al. Functional organ preservation with definitive chemoradiotherapy for T4 laryngeal squamous cell carcinoma. Ann Oncol 2008;19(9):1650–4.
[6] Worden FP, Moyer J, Lee JS, et al. Chemoselection as a strategy for organ preservation in patients with T4 laryngeal squamous cell carcinoma with cartilage invasion. Laryngoscope 2009;119(8):1510–7.
[7] Castelijns JA, Becker M, Hermans R. Impact of cartilage invasion on treatment and prognosis of laryngeal cancer. Eur Radiol 1996;6(2):156–69.
[8] Hermans R. Staging of laryngeal and hypopharyngeal cancer: value of imaging studies. Eur Radiol 2006;16(11):2386–400.
[9] Li B, Bobinski M, Gandour-Edwards R, Farwell DG, Chen AM. Overstaging of cartilage invasion by multidetector CT scan for laryngeal cancer and its potential effect on the use of organ preservation with chemoradiation. Br J Radiol 2011;84(997):64–9.
[10] Hartl DM, Landry G, Hans S, Marandas P, Brasnu DF. Organ preservation surgery for laryngeal squamous cell carcinoma: low incidence of thyroid cartilage invasion. Laryngoscope 2010;120(6):1173–6.
[11] Graser A, Johnson TR, Hecht EM, et al. Dual-energy CT in patients suspected of having renal masses: can virtual nonenhanced images replace true nonenhanced images? Radiology 2009;252(2):433–40.
[12] Gupta R, Phan CM, Leidecker C, et al. Evaluation of dual-energy CT for differentiating intracerebral hemorrhage from iodinated contrast material staining. Radiology 2010;257(1):205–11.
[13] Johnson TR, Krauss B, Sedlmair M, et al. Material differentiation by dual energy CT: initial experience. Eur Radiol 2007;17(6):1510–7.
[14] Kang MJ, Park CM, Lee CH, Goo JM, Lee HJ. Dual-energy CT: clinical applications in various pulmonary diseases. Radiographics 2010;30(3):685–98.

[15] Leschka S, Stolzmann P, Baumuller S, et al. Performance of dual-energy CT with tin filter technology for the discrimination of renal cysts and enhancing masses. Acad Radiol 2010;17(4):526–34.
[16] Kuno H, Onaya H, Iwata R, et al. Evaluation of cartilage invasion by laryngeal and hypopharyngeal squamous cell carcinoma with dual-energy CT. Radiology 2012;265(2):488–96.
[17] Sulfaro S, Barzan L, Querin F, et al. T staging of the laryngohypopharyngeal carcinoma. A 7-year multidisciplinary experience. Arch Otolaryngol Head Neck Surg 1989;115(5):613–20.
[18] Zbaren P, Becker M, Lang H. Pretherapeutic staging of laryngeal carcinoma. Clinical findings, computed tomography, and magnetic resonance imaging compared with histopathology. Cancer 1996;77(7):1263–73.
[19] Becker M, Burkhardt K, Dulguerov P, Allal A. Imaging of the larynx and hypopharynx. Eur J Radiol 2008;66(3):460–79.
[20] Edge SB BD, Compton CC, et al. (edrs) AJCC Cancer Staging Handbook (ed 7), New York, NY, Springer2010.
[21] Mendenhall WM, Parsons JT, Mancuso AA, Pameijer FJ, Stringer SP, Cassisi NJ. Definitive radiotherapy for T3 squamous cell carcinoma of the glottic larynx. J Clin Oncol 1997;15(6):2394–402.
[22] Mendenhall WM, Werning JW, Hinerman RW, Amdur RJ, Villaret DB. Management of T1–T2 glottic carcinomas. Cancer 2004;100(9):1786–92.
[23] Murakami R, Nishimura R, Baba Y, et al. Prognostic factors of glottic carcinomas treated with radiation therapy: value of the adjacent sign on radiological examinations in the sixth edition of the UICC TNM staging system. Int J Radiat Oncol Biol Phys 2005;61(2):471–5.
[24] Baum U, Greess H, Lell M, Nomayr A, Lenz M. Imaging of head and neck tumors - methods: CT, spiral-CT, multislice-spiral-CT. Eur J Radiol 2000;33(3):153–60.
[25] Lell MM, Greess H, Hothorn T, Janka R, Bautz WA, Baum U. Multiplanar functional imaging of the larynx and hypopharynx with multislice spiral CT. Eur Radiol 2004;14(12):2198–205.
[26] Becker M, Zbaren P, Delavelle J, et al. Neoplastic invasion of the laryngeal cartilage: reassessment of criteria for diagnosis at CT. Radiology 1997;203(2):521–32.
[27] Brown CL, Hartman RP, Dzyubak OP, et al. Dual-energy CT iodine overlay technique for characterization of renal masses as cyst or solid: a phantom feasibility study. Eur Radiol 2009;19(5):1289–95.
[28] Karlo C, Lauber A, Gotti RP, et al. Dual-energy CT with tin filter technology for the discrimination of renal lesion proxies containing blood, protein, and contrast-agent. An experimental phantom study Eur Radiol 2011;21(2):385–92.
[29] Alvarez RE, Macovski A. Energy-selective reconstructions in X-ray computerized tomography. Phys Med Biol 1976;21(5):733–44.
[30] Hounsfield GN. Computerized transverse axial scanning (tomography). 1. Description of system. Br J Radiol 1973;46(552):1016–22.
[31] Kalender WA, Perman WH, Vetter JR, Klotz E. Evaluation of a prototype dual-energy computed tomographic apparatus.1. Phantom studies. Med Phys 1986;13(3):334–9.
[32] Kaza RK, Platt JF, Cohan RH, Caoili EM, Al-Hawary MM, Wasnik A. Dual-energy CT with single- and dual-source scanners: current applications in evaluating the genitourinary tract. Radiographics 2012;32(2):353–69.
[33] Krauss B, Schmidt B, Flohr T. Dual source CT. In: Johnson TRC, Fink C, Schönberg SO, Reiser MF, editors. Dual energy CT in clinical practice. 1st ed. Heidelberg, Dordrecht, London, New York: Springer; 2011. p. 11–20.
[34] Flohr TG, McCollough CH, Bruder H, et al. First performance evaluation of a dual-source CT (DSCT) system. Eur Radiol 2006;16(2):256–68.
[35] Tawfik AM, Kerl JM, Razek AA, et al. Image quality and radiation dose of dual-energy CT of the head and neck compared with a standard 120-kVp acquisition. AJNR Am J Neuroradiol 2011;32(11):1994–9.
[36] Paul J, Bauer RW, Maentele W, Vogl TJ. Image fusion in dual energy computed tomography for detection of various anatomic structures—effect on contrast enhancement, contrast-to-noise ratio, signal-to-noise ratio and image quality. Eur J Radiol 2011.
[37] Becker M. Neoplastic invasion of laryngeal cartilage: radiologic diagnosis and therapeutic implications. Eur J Radiol 2000;33(3):216–29.
[38] Becker M, Zbaren P, Laeng H, Stoupis C, Porcellini B, Vock P. Neoplastic invasion of the laryngeal cartilage: comparison of MR imaging and CT with histopathologic correlation. Radiology 1995;194(3):661–9.
[39] Beitler JJ, Muller S, Grist WJ, et al. Prognostic accuracy of computed tomography findings for patients with laryngeal cancer undergoing laryngectomy. J Clin Oncol 2010;28(14):2318–22.
[40] Nix PA, Salvage D. Neoplastic invasion of laryngeal cartilage: the significance of cartilage sclerosis on computed tomography images. Clin Otolaryngol Allied Sci 2004;29(4):372–5.
[41] Schmalfuss IM, Mancuso AA, Tart RP. Arytenoid cartilage sclerosis: normal variations and clinical significance. AJNR Am J Neuroradiol 1998;19(4):719–22.
[42] Munoz A, Ramos A, Ferrando J, et al. Laryngeal carcinoma: sclerotic appearance of the cricoid and arytenoid cartilage—CT-pathologic correlation. Radiology 1993;189(2):433–7.
[43] Gilbert K, Dalley RW, Maronian N, Anzai Y. Staging of laryngeal cancer using 64-channel multidetector row CT: comparison of standard neck CT with dedicated breath-maneuver laryngeal CT. Am J Neuroradiol 2010;31(2):251–6.
[44] Castelijns JA, Gerritsen GJ, Kaiser MC, et al. Invasion of laryngeal cartilage by cancer: comparison of CT and MR imaging. Radiology 1988;167(1):199–206.
[45] Becker M, Zbaren P, Casselman JW, Kohler R, Dulguerov P, Becker CD. Neoplastic invasion of laryngeal cartilage: reassessment of criteria for diagnosis at MR imaging. Radiology 2008;249(2):551–9.
[46] Hermans R, VanderGoten A, Baert AL. Image interpretation in CT of laryngeal carcinoma: a study on intra- and interobserver reproducibility. Eur Radiol 1997;7(7):1086–90.
[47] Hoorweg JJ, Kruijt RH, Heijboer RJJ, Eijkemans MJC, Kerrebijn JDF. Reliability of interpretation of CT examination of the larynx in patients with glottic laryngeal carcinoma. Otolaryngol Head Neck Surg 2006;135(1):129–34.
[48] Mancuso AA. Hypopharynx: malignant tumors. In: Mancuso AA, Hanafee WN, editors. Head and neck radiology. Philadelphia: Lippincott Williams & Wilkins; 2010. p. 2147–72.
[49] Mancuso AA. Larynx: malignant tumors. In: Mancuso AA, Hanafee WN, editors. Head and neck radiology. Philadelphia: Lippincott Williams & Wilkins; 2010. p. 1975–2022.
[50] Zbaren P, Egger C. Growth patterns of piriform sinus carcinomas. Laryngoscope 1997;107(4):511–8.

J Gastroenterol (2014) 49:932–940
DOI 10.1007/s00535-013-0853-7

The Japanese Society of Gastroenterology

ORIGINAL ARTICLE—LIVER, PANCREAS, AND BILIARY TRACT

Efficacy of sorafenib in patients with hepatocellular carcinoma refractory to transcatheter arterial chemoembolization

Masafumi Ikeda · Shuichi Mitsunaga · Satoshi Shimizu · Izumi Ohno · Hideaki Takahashi · Hiroyuki Okuyama · Akiko Kuwahara · Shunsuke Kondo · Chigusa Morizane · Hideki Ueno · Mitsuo Satake · Yasuaki Arai · Takuji Okusaka

Received: 5 March 2013 / Accepted: 9 June 2013 / Published online: 23 June 2013

Abstract
Background The efficacy of sorafenib for hepatocellular carcinoma (HCC) patients refractory to transcatheter arterial chemoembolization (TACE) has not yet been clarified. We investigated the efficacy of sorafenib in HCC patients who were refractory to TACE (sorafenib group) and retrospectively compared the results with those of patients treated with hepatic arterial infusion chemotherapy using cisplatin (cisplatin group).
Methods We evaluated the anti-tumor effect, the time to progression, and the overall survival in 48 patients in the sorafenib group and 66 patients in the cisplatin group.
Results The disease control rate to sorafenib was 60.4 %, the median time to progression was 3.9 months, and the median survival time was 16.4 months in patients who were refractory to TACE. When compared with the cisplatin group, significant differences in the patient characteristics were not observed between the two groups with the exception of patient age; however, the disease control rate (cisplatin group 28.8 %, $P = 0.001$), time to progression (cisplatin group: median 2.0 months, hazard ratio 0.44, $P < 0.01$), and overall survival (cisplatin group: median 8.6 months, hazard ratio 0.57, $P < 0.001$) were significantly superior in the sorafenib group. The multivariate analysis also showed the sorafenib treatment to be the most significant factor contributing to prolongation of time to progression and overall survival.
Conclusions Sorafenib showed favorable treatment results in patients refractory to TACE. When compared with hepatic arterial infusion chemotherapy using cisplatin, sorafenib demonstrated a significantly higher disease control rate, a longer time to progression and increased overall survival.

Keywords Hepatocellular carcinoma · Sorafenib · Cisplatin · Chemotherapy · Hepatic arterial infusion chemotherapy

M. Ikeda (✉) · S. Mitsunaga · S. Shimizu · I. Ohno · H. Takahashi · H. Okuyama · A. Kuwahara
Division of Hepatobiliary and Pancreatic Oncology, National Cancer Center Hospital East, 6-5-1 Kashiwanoha, Kashiwa, Chiba 277-8577, Japan
e-mail: masikeda@east.ncc.go.jp

S. Kondo · C. Morizane · H. Ueno · T. Okusaka
Hepatobiliary and Pancreatic Oncology Division, National Cancer Center Hospital, Tokyo, Japan

M. Satake
Division of Diagnostic Radiology, National Cancer Center Hospital East, Kashiwa, Japan

Y. Arai
Department of Diagnostic Radiology, National Cancer Center Hospital, Tokyo, Japan

Introduction

Hepatocellular carcinoma (HCC) is one of the most common malignancies worldwide. HCC is highly prevalent in African and Asian countries, and its incidence has recently been increasing in western countries [1, 2]. For patients with unresectable HCC who are not candidates for curative treatments, such as resection, transplantation, or local ablation, transcatheter arterial chemoembolization (TACE) is the main therapeutic option [1, 2]. A clear survival benefit for patients with unresectable HCC who are treated with TACE has been shown in several randomized controlled trials and a meta-analysis [3, 4]. Chemotherapy has been recognized as a palliative treatment option for patients with highly advanced HCC in whom TACE is not indicated.

Sorafenib is a multikinase inhibitor of Raf kinase, which is involved in cancer cell proliferation, as well as vascular

endothelial growth factor receptor-2/-3 (VEGFR-2/-3) and platelet-derived growth factor receptor beta (PDGFR-β), which is involved in peritumor neovascularization [5, 6]. In two pivotal international phase 3 trials of sorafenib vs. placebo, the so-called SHARP trial [7] and the Asia-Pacific trial [8], sorafenib demonstrated a prolonged overall survival and time-to-progression, compared with a placebo, in patients with advanced hepatocellular carcinoma (HCC). Therefore, sorafenib has been acknowledged as a standard therapy for advanced HCC.

In the therapeutic strategy of the Barcelona Clinic Liver Cancer Study Group [5], sorafenib was indicated for patients with extrahepatic metastasis and/or vascular invasion of Stage C disease (advanced stage), patients with a performance status (PS) of 1–2, and those with Stage B (intermediate stage) multifocal HCC refractory to TACE. In the 2010 updated version of the consensus-based clinical practice guidelines for the management of HCC proposed by the Japan Society of Hepatology [9, 10], patients with extrahepatic metastasis, with macrovascular invasion, and who were refractory to TACE are listed in the algorithm for treatment with sorafenib. The main indications for sorafenib are, therefore, considered to be patients who are refractory to TACE, those who have vascular invasion, or those who have extrahepatic metastasis. Subgroup analyses of the SHARP trial [7] and the Asia-Pacific trial [8] showed the treatment efficacies in patients with vascular invasion and extrahepatic metastasis. However, those in patients who are refractory to TACE have not been reported so far, although the outcome of patients with prior TACE has been reported [11, 12].

Before the introduction of sorafenib, hepatic arterial infusion chemotherapy was mainly performed in Japan for patients with advanced HCC [13–21], including those refractory to TACE [13, 14]. However, no consensus on a standard therapy has been achieved because large-scale prospective studies and randomized controlled studies have not been conducted and the survival benefit has not been clarified [10]. In this study, we clarified the efficacy of sorafenib in patients who were refractory to TACE (sorafenib group) and retrospectively compared the anti-tumor effect, time to progression, and overall survival between the sorafenib group and patients who were refractory to TACE and who were treated with hepatic arterial infusion chemotherapy using cisplatin (cisplatin group).

Patients and methods

Patients

Forty-eight consecutive chemotherapy-naive patients who were refractory to TACE without extrahepatic metastasis were extracted from 205 patients treated with sorafenib at the National Cancer Center Hospital East (East Hospital) between April 2009 and December 2011. Sixty-six of the 84 chemo-naive patients who were refractory to TACE and were treated with hepatic arterial infusion chemotherapy using cisplatin at the National Cancer Center Hospital and the East Hospital between July 2004 and September 2008, the period before the approval of sorafenib in Japan, were enrolled in the cisplatin group after excluding 18 patients with extrahepatic metastasis or the moderate retention of ascites. In this series, the total number of TACE sessions was 478, while the median number of TACE sessions was 4 (range 1–16). In previous TACE sessions, an emulsion containing an anticancer agent and lipiodol followed by gelatin sponge particles were used. In the present series, epirubicin was used for 394 sessions, adriamycin was used for 29 sessions, and mitomycin C was used for 12 sessions; the anticancer agent was unknown for 43 sessions. Patients who were refractory to TACE were defined as those showing progression or a tumor shrinkage rate of <25 % of the hypervascular lesions as visualized using dynamic computed tomography (CT) and/or magnetic resonance imaging (MRI) after 1–3 months of TACE [13]. The TACE-refractory status of individual patients was discussed at a weekly tumor board conference. HCC was diagnosed based on the presence of histopathological findings or imaging findings that were characteristic of HCC together with an increase in the serum α-fetoprotein level. The diameter of the tumor and the presence/absence of extrahepatic metastasis were confirmed using dynamic CT/MRI, ultrasound, or chest X-ray/CT prior to treatment. In our hospital, sorafenib is indicated for the treatment of patients with highly advanced HCC with a Child–Pugh score of either A or B. Informed consent for each treatment was obtained from all the patients before the initiation of treatment. This clinical study was conducted with the approval of the Ethics Committee of the National Cancer Center and was conducted in accordance with the ethical principals stated in the Japanese ethics guideline for epidemiological research.

Treatments

An oral dose of sorafenib at 400 mg was administered twice daily, after breakfast and dinner (800 mg/day). Treatment was continued as long as tolerability was observed without obvious disease progression. The dose was reduced or withdrawn and treatment was continued depending on the severity of adverse events. A dose increase up to 800 mg/day was permitted when the dose increase was judged possible in patients in whom the dose had been reduced.

For hepatic arterial infusion chemotherapy using cisplatin, intra-arterial cisplatin at a dose of 65 mg/m^2 was

administered over 20–40 min via a catheter inserted into the feeding arteries of the tumors. Treatment was repeated every 4–6 weeks for up to 6 courses until disease progression or unacceptable toxicities occurred. An infusion of 3,000 mL or more was administered on the day of treatment, and an infusion of 1,000 mL or more was continued for 3 days after administration to reduce renal toxicity caused by cisplatin; a diuretic (mannitol, furosemide, etc.) was administered as necessary to ensure an adequate urine volume.

Assessment and statistical analyses

Dynamic CT or MRI was used to confirm the anti-tumor effect every 1–2 months. The anti-tumor effect was evaluated using the Response Evaluation Criteria in Solid Tumors, version 1.0 (RECIST) [22], to judge the best overall response. The time to progression was defined as the period from the date of the start of treatment until the date of the confirmation of tumor progression by radiological evaluation or the day on which obvious tumor progression was judged to have occurred based on the clinical symptoms. Overall survival was defined as the period from the day of the start of treatment until the date of death or the final date of confirmed survival. A χ^2 test or Wilcoxon test was used to compare the patient characteristics and the anti-tumor effect between the sorafenib and the hepatic arterial infusion chemotherapy using cisplatin groups, and the Kaplan–Meier method was used to calculate the time to progression and the overall survival; the log-rank test was used to analyze differences between the groups. In a multivariate analysis, a Cox regression was used to analyze factors with $P < 0.10$ using a univariate analysis. $P < 0.05$ was judged to be statistically significant. JMP version 9.0 (SAS Institute Inc.) was used for the above statistical analyses.

Results

Patient characteristics

Table 1 shows the patient characteristics before each treatment. Age was significantly higher in the sorafenib group, although the medians were very similar (sorafenib group 71 years, cisplatin group 69 years). Although the Eastern Cooperative Oncology Group PS, the maximum tumor diameter, total bilirubin, AST, and ALT tended to be slightly worse in the cisplatin group, significant differences were not observed in the other parameters between the two groups. The median number of treatments in the cisplatin group was 2 (range 1–6 times). As a subsequent treatment, other systemic chemotherapy was performed in 14 patients, hepatic arterial infusion chemotherapy using cisplatin was performed in 7 patients, TACE was performed in 4 patients, and hepatic arterial infusion chemotherapy using 5-FU + interferon and radiotherapy was performed in one patient each in the sorafenib group; meanwhile, TACE was performed in 15 patients, hepatic arterial infusion chemotherapy using epirubicin was performed in 4 patients, other systemic chemotherapy was performed in 4 patients, hepatic arterial infusion chemotherapy using 5-FU + interferon was performed in 2 patients, and radiotherapy was performed in one patient in the cisplatin group. The median observation period was 9.4 months (range 2.1–31.6 months) in the sorafenib group and 7.5 months (range 0.8–43.1 months) in the cisplatin group; this difference was not statistically significant ($P = 0.44$).

Efficacy

The best overall response in the sorafenib group was evaluated as a complete response (CR) in one patient, a partial response (PR) in 2 patients, stable disease (SD) in 26 patients, progressive disease (PD) in 16 patients, and not evaluable (NE) in 3 patients. The response rate (CR + PR) was 6.3 % [95 % confidence interval (CI) 1.3–17.2 %], and the disease control rate (CD + PR + SD) was 60.4 % (95 % CI 45.3–74.2 %). The median time to progression and the progression-free rate at 6- and 12-months were 3.9 months, 32.6 %, and 12.1 %, respectively, while the median overall survival and the survival rate at 6-, 12-, and 24-months was 16.4 months, 88.9 %, 55.3 %, and 32.5 %, respectively, in the sorafenib group.

The best overall response in the cisplatin group was evaluated as a CR in 1 patient, PR in 0 patients, SD in 18 patients, PD in 39 patients, and NE in 8 patients. The response rate was 1.5 % (95 % CI 0.04–8.2 %), and a significant difference in the response rate, compared with the sorafenib group, was not observed ($P = 0.40$). The disease control rate was 28.8 % (95 % CI 18.3–41.3 %), which was significantly higher in the sorafenib group ($P = 0.001$). The median time to progression and the progression-free rate at 6- and 12-months in the cisplatin group was 2.0 months, 15.9 %, and 4.8 %, respectively, showing a significantly superior result in the sorafenib group (hazard ratio 0.44, $P < 0.01$) (Fig. 1). At the time of analysis, 21 patients had died because of tumor progression, and 1 patient had died because of hepatic failure in the sorafenib group. Additionally, 60 patients had died because of tumor progression, and 4 patients had died because of hepatic failure in the cisplatin group. The median survival time and the survival rate at 6-, 12-, and 24-months in the cisplatin group were 8.6 months, 62.0 %, 35.2 %, and 11.3 %, respectively, showing a significantly superior result in the sorafenib group (hazard ratio: 0.57,

Table 1 Patient characteristics

	Sorafenib		Cisplatin		*P* value
	n	(%)	*n*	(%)	
All patients	48	–	66	–	
Age (years)					
Median [range]	71	[53–83]	69	[40–82]	0.04
Sex					
Male	43	(90)	52	(79)	
Female	5	(10)	14	(21)	1.00
Performance status					
0	43	(90)	49	(74)	
1	5	(10)	17	(26)	0.07
HCVAb (positive)	32	(67)	45	(68)	1.00
HBsAg (positive)	7	(15)	8	(12)	0.92
Prior resection (present)	12	(25)	27	(41)	0.11
Prior ablation (present)	19	(40)	29	(44)	1.00
No. of prior TACE sessions					
Median [range]	4	[1–9]	4	[1–17]	0.86
Maximum tumor diameter (mm)					
Median [range]	30.5	[10–150]	40	[12–110]	0.07
Number of tumors					
1–3	8	(17)	13	(20)	0.32
≥4	40	(83)	53	(80)	0.64
Portal vein invasion (present)	9	(19)	16	(24)	0.64
Hepatic vein invasion (present)	3	(6)	4	(6)	0.99
Stage[a]					
II or III	38	(79)	49	(74)	
IVa	10	(21)	17	(26)	0.70
Ascites (present)	9	(19)	17	(26)	0.51
Child–Pugh class					
A	32	(67)	36	(55)	
B	16	(33)	30	(45)	0.27
Total bilirubin (mg/dL)					
Median [range]	0.9	[0.3–2.1]	1.1	[0.2–3.0]	0.02
Albumin (g/dL)					
Median [range]	3.5	[2.3–4.8]	3.3	[2.4–4.5]	0.21
AST (U/L)					
Median [range]	54	[20–165]	88	[35–287]	0.04
ALT (U/L)					
Median [range]	43	[10–139]	62	[22–187]	0.05
Prothrombin time (%)					
Median [range]	78	[40–107]	73	[48–104]	0.39
α-Fetoprotein (ng/mL)					
Median [range]	70.3	[1.3–218876]	324.3	[1.7–210200]	0.59
PIVKAII (mAU/mL)					
Median [range]	505.5	[11–291330]	438	[11–96390]	0.65
Subsequent treatments (present)	27	(56)	26	(39)	0.11

HCVAb hepatitis C viral antibody, *HBsAg* hepatitis B surface antigen, *TACE* transcatheter arterial chemoembolization, *AST* aspartate aminotransferase, *ALT* alanine aminotransferase, *PIVKAII* protein induced by vitamin K absence or antagonists-II

[a] Japanese classification of primary liver cancer

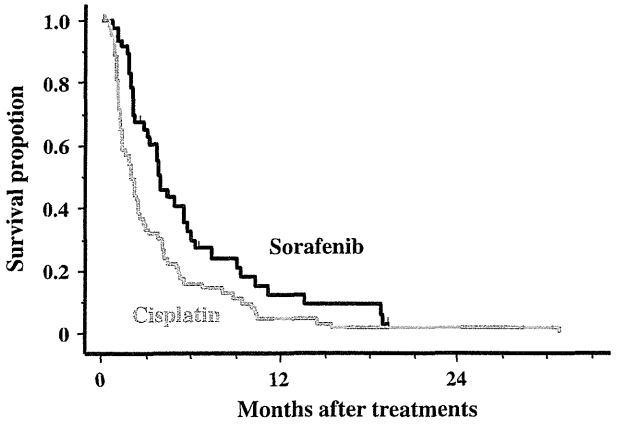

Fig. 1 Comparison of time to progression between sorafenib and hepatic arterial infusion chemotherapy using cisplatin in patients who were refractory to transcatheter arterial chemoembolization (TACE)

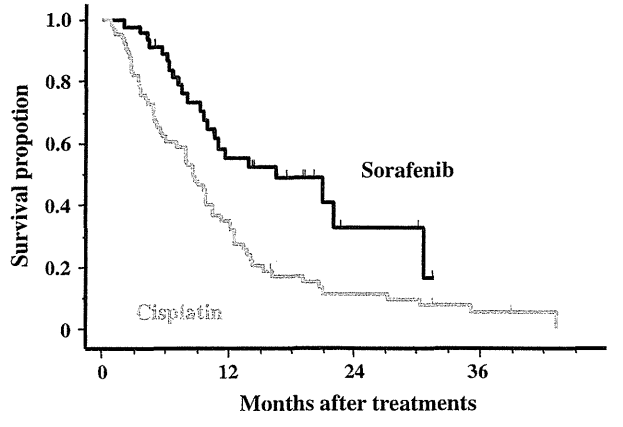

Fig. 2 Comparison of overall survival between sorafenib and hepatic arterial infusion chemotherapy using cisplatin in patients who were refractory to TACE

$P < 0.001$) (Fig. 2). The same analysis was performed for patients limited to Child–Pugh A, since sorafenib is widely recommended for the treatment of patients with Child–Pugh A. The results were similar, although the disease control rate and the time to progression were not statistically significant (data not shown).

Toxicity

Serious adverse events (SAE) occurred in two patients (1 patient, grade 4 hepatic encephalopathy; 1 patient, grade 3 erythema multiforme) in the sorafenib group, but none of the patients in the cisplatin group experienced an SAE. Thirty-eight patients (79 %) required a sorafenib dose reduction because of adverse events, such as liver dysfunction, hand-foot syndrome, or rashes, and treatment was discontinued in 7 patients (14 %) because of adverse events, such as liver dysfunction, hepatic encephalopathy, or erythema multiforme. On the other hand, none of the patients required a cisplatin dose reduction, and treatment was discontinued in 6 patients (9.1 %) because of adverse events, such as liver dysfunction, fatigue, or nausea/anorexia.

Predictive factors of time to progression and overall survival

Univariate analyses were performed to identify the factors that contributed to the prolongation of time to progression in patients who were refractory to TACE (Table 2). The univariate analyses showed that the significant factors that contributed to the prolongation of the time to progression ($P < 0.10$) were an age >65 years, a PS of 0, a maximum tumor diameter ≤3.0 cm, the absence of hepatic vein invasion, the absence of ascites, a bilirubin level ≤1.2 mg/dL, an α-fetoprotein level <1,000 ng/mL, and sorafenib treatment. A multivariate analysis was performed for the factors that showed a significant tendency ($P < 0.10$) in the univariate analysis, and the absence of hepatic vein invasion and sorafenib treatment were significant independent factors that contributed to the prolongation of the time to progression (Table 3). Univariate analyses were performed to identify the factors that contributed to survival prolongation in patients who were refractory to TACE (Table 2). The univariate analyses showed that the significant factors that contributed to the prolongation of survival ($P < 0.10$) were an age >65 years, a PS of 0, a maximum tumor diameter of ≤3.0 cm, 3 or fewer tumors, the absence of hepatic vein invasion, Child–Pugh class A, the absence of ascites, an albumin level >3.5 g/dL, a bilirubin level ≤1.2 mg/dL, an AST level <100 U/L, an α-fetoprotein level <1,000 ng/mL, a protein induced by vitamin K absence or antagonist-II (PIVKA-II) level <1,000 mAU/mL, and sorafenib treatment. A multivariate analysis was performed for the factors showing a significant tendency at $P < 0.10$, and the significant independent favorable prognosis factors were a PS of 0, 3 or fewer tumors, Child–Pugh A, an α-fetoprotein level <1,000 ng/mL, a PIVKA-II level <1,000 mAU/mL, and treatment with sorafenib (Table 3). Treatment with sorafenib had the smallest hazard ratio among these prognostic factors.

Discussion

Patients with vascular invasion, extrahepatic metastasis, and who are refractory to TACE are good candidates for sorafenib [5, 9, 10]. However, the efficacy of sorafenib in patients who are refractory to TACE has not been previously reported, although the outcome of patients with prior

Table 2 Univariate analysis of time to progression and overall survival time in patients refractory to transcatheter arterial chemoembolization treated with sorafenib or intra-arterial cisplatin

	n	Time to progression			Overall survival		
		Median (months)	Hazard ratio	*P* value	Median (months)	Hazard ratio	*P* value
Sex							
Female	19	2.9	1.01 (0.60–1.68)	0.98	10.5	0.92 (0.51–1.68)	0.79
Male	95	2.6			9.8		
Age (years)							
≤65	33	2.0	1.41 (0.92–2.14)	0.11	8.0	1.65 (1.03–2.66)	0.03
>65	81	3.0			11.4		
Performance status							
0	92	3.2	0.58 (0.35–0.95)	0.03	11.4	0.38 (0.22–0.66)	<0.001
1–2	22	1.6			4.8		
HCVAb							
Negative	37	2.8	0.82 (0.53–1.25)	0.35	9.9	0.72 (0.45–1.18)	0.19
Positive	77	2.5			9.8		
HBsAg							
Negative	99	3.0	0.86 (0.50–1.50)	0.60	9.9	1.09 (0.54–2.17)	0.82
Positive	15	2.1			9.8		
Maximum tumor diameter (cm)							
≤3.0	39	4.0	0.65 (0.43–0.99)	0.04	12.3	0.56 (0.34–0.83)	0.02
>3.0	75	2.2			8.7		
No. of tumors							
≤3	21	4.4	0.78 (0.48–1.29)	0.33	13.8	0.68 (0.39–1.19)	0.06
>3	93	2.4			8.0		
Portal vein invasion							
Present	25	3.2	0.89 (0.55–1.43)	0.62	5.4	1.34 (0.79–2.27)	0.23
Absent	89	2.6			8.7		
Hepatic vein invasion							
Present	7	2.5	2.12 (0.97–4.66)	0.05	4.8	2.17 (0.94–5.03)	0.13
Absent	107	2.8			9.2		
Stage[a]							
II or III	87	2.8	0.94 (0.59–1.48)	0.77	11.6	0.64 (0.39–1.07)	0.08
IV	27	2.5			6.2		
Child–Pugh class							
A	68	3.2	0.84 (0.56–1.26)	0.39	9.5	0.65 (0.41–1.01)	0.08
B	46	2.2			7.8		
Ascites							
Present	26	2.2	1.56 (0.98–2.47)	0.06	5.6	2.15 (1.32–3.53)	0.01
Absent	88	2.9			9.2		
Albumin (g/dL)							
≤3.5	76	2.4	1.17 (0.78–1.77)	0.44	7.8	1.90 (1.16–3.11)	0.02
>3.5	38	3.8			10.6		
Total bilirubin (mg/dL)							
≤1.2	81	3.2	0.66 (0.42–1.02)	0.06	11.6	0.42 (0.26–0.66)	<0.001
>1.2	33	1.6			4.8		
Prothrombin time (%)							
<70	42	2.9	0.95 (0.63–1.42)	0.79	10.5	0.93 (0.59–1.47)	0.77
≥70	72	2.5			9.9		

Table 2 continued

	n	Time to progression			Overall survival		
		Median (months)	Hazard ratio	*P* value	Median (months)	Hazard ratio	*P* value
AST (U/L)							
<100	82	3.0	0.86 (0.55–1.35)	0.50	12.3	0.44 (0.27–0.70)	<0.001
≥100	32	2.2			5.5		
ALT (U/L)							
<100	97	2.6	0.90 (0.52–1.56)	0.70	9.9	0.85 (0.44–1.57)	0.59
≥100	17	2.5			8.5		
α-Fetoprotein (ng/mL)							
<1,000	71	3.8	0.60 (0.40–0.91)	0.01	12.2	0.61 (0.39–0.96)	0.03
≥1,000	43	2.1			7.1		
PIVKA-II (mAU/mL)							
<1,000	67	3.1	0.78 (0.52–1.16)	0.22	10.6	0.62 (0.40–0.96)	0.03
≥1,000	45	2.1			9.5		
Treatments							
Sorafenib	48	3.9	0.57 (0.38–0.86)	0.01	16.4	0.44 (0.27–0.72)	<0.001
Cisplatin	66	2.0			8.6		

HCVAb hepatitis C viral antibody, *HBsAg* hepatitis B surface antigen, *AST* aspartate aminotransferase, *ALT* alanine aminotransferase, *PIVKAII* protein induced by vitamin K absence or antagonists-II

[a] Japanese classification of primary liver cancer

Table 3 Multivariate analysis of overall survival and time to progression in patients refractory to TACE

	Hazard ratio	*P* value
Time to progression		
Hepatic vein invasion: present	0.41 (0.19–0.91)	0.03
Treatment: sorafenib	0.55 (0.37–0.83)	0.004
Overall survival		
Performance status: 0	0.46 (0.27–0.81)	0.006
No. of tumors: ≤3	0.51 (0.29–0.91)	0.02
Child–Pugh class: A	0.44 (0.27–0.71)	0.001
α-Fetoprotein: <1,000 ng/mL	0.52 (0.22–0.84)	0.008
PIVKA-II: <1,000 mAU/mL	0.47 (0.29–0.76)	0.002
Treatment: sorafenib	0.42 (0.25–0.77)	0.001

TACE has been reported [11, 12]. We retrospectively evaluated the efficacy of sorafenib in patients who were refractory to TACE. The following data were obtained: the response rate (CR + PR) was 6.3 %, the disease control rate (CD + PR + SD) was 60.4 %, and the median time to progression was 3.9 months; these results were comparable to those obtained for sorafenib to date [7, 8]. The median survival time of 16.4 months was regarded as favorable. The patients who were refractory to TACE have a lower frequency of vascular invasion, which is a significant predictor of a poor prognosis in patients with advanced HCC. In addition, most of the TACE refractory patients had an intermediate BCLC stage. The TACE refractory patients in this study (proportion of advanced stage 33 %) had a better BCLC stage than the patients in previous trials (proportion of advanced stage SHARP, 82 %; Asia-Pacific trial, 95.3 %). Favorable tendencies, therefore, might be shown for the overall survival of a subgroup of patients who are refractory to TACE among advanced HCC patients in whom sorafenib treatment is indicated.

A definition of "refractory to TACE" has not yet been established. In this study, the definition of "refractory to TACE" was regarded as progression or a tumor shrinkage rate of <25 % in hypervascular lesions as visualized using dynamic CT and/or MRI after 1–3 months of TACE. According to the consensus-based clinical practice guidelines proposed by the Japan Society of Hepatology 2010 [5], however, "refractory to TACE" is defined as two or over consecutive incomplete necrotic reactions or the appearance of a new lesion, vascular invasion, or extrahepatic metastases. Although a consensus has not been reached among clinicians, this is a critical issue when considering a conversion from TACE to sorafenib treatment in patients with unresectable HCC.

In the present study, sorafenib was compared with hepatic arterial infusion chemotherapy using cisplatin, which was used before the introduction of sorafenib. A consensus on a standard therapy has not been attained for hepatic arterial infusion chemotherapy, since its survival benefit has not been elucidated [10]. However, this regimen is still frequently used in Japan, because favorable antitumor effects and long-term survivals have been seen in a

few patients [15–21]. Nonetheless, hepatic arterial infusion chemotherapy has not been reported to have favorable results in patients who are refractory to TACE [13, 14]. Regarding hepatic arterial infusion chemotherapy using cisplatin in patients who were refractory to TACE ($n = 84$), the response rate at out-patient hospitals was 3.6 %, the median time to progression was 1.7 months, and the median overall survival period was 7.1 months [13], while the results of a phase II study of hepatic arterial infusion chemotherapy using cisplatin in patients with unresectable HCC ($n = 80$) were favorable, with a response rate of 33.8 % and a 1-year survival rate of 67.5 % [15]. One possible reason for the difference between these studies might be differences in the characteristics of the study populations. Most patients in the phase II trial of cisplatin were TACE-naïve, whereas only patients with TACE-refractory disease were included in the present study. Thus, hepatic arterial infusion chemotherapy may not be expected to show favorable therapeutic results when the patients are limited to those refractory to TACE, although the reason remains unknown. Therefore, the results were compared with those for patients who were refractory to TACE and were treated with sorafenib. Although the patient age was significantly higher in the sorafenib group and the PS and tumor size was slightly worse in the cisplatin group, no other significant differences in the patient characteristics were observed between the two groups. The response rate was comparable, but the sorafenib group showed significantly higher results for the disease control rate, time to progression, and overall survival. We also performed a multivariate analysis to examine the factors that contributed to the time to progression and overall survival in patients who were refractory to TACE, and treatment with sorafenib was one of the significant factors. These results suggest that sorafenib, rather than hepatic arterial infusion chemotherapy using cisplatin, might be the treatment of first choice in patients who are refractory to TACE. This outcome might not have much impact in overseas settings, where hepatic arterial infusion chemotherapy is less popular, but it is quite disappointing in Japan, since hepatic arterial infusion chemotherapy using cisplatin was expected to show a therapeutic effect comparable to that of sorafenib.

The present study has some limitations. First, the results for sorafenib treatment in patients who were refractory to TACE were obtained as part of a single-site, retrospective study. A prospective study enrolling only patients who are refractory to TACE should be performed in the future to verify the efficacy of sorafenib in patients who are refractory to TACE. Second, the periods of treatment differed between the sorafenib group and the cisplatin group. Third, the influence of subsequent treatment on the overall survival cannot be denied. Hepatic arterial infusion chemotherapy using cisplatin was administered as a subsequent treatment in 7 patients in the sorafenib group, whereas patients in the cisplatin group were not treated with sorafenib. Still, the anti-tumor effect of hepatic arterial infusion chemotherapy using cisplatin following sorafenib was PD in all the patients, and the impact would have been negligible. Finally, considering the possible selection bias in therapeutic policy after the introduction of sorafenib, we selected patients with different periods of treatment, but the results might also have been affected by the difference in periods. Also, no significant differences in the patient characteristics, except for age, total bilirubin, and AST, were seen between the sorafenib and the hepatic arterial infusion chemotherapy using cisplatin group, but subtle differences in the patient characteristics might have affected the favorable results for sorafenib, since this study was a retrospective comparison.

In conclusion, sorafenib showed a favorable efficacy in patients who were refractory to TACE, resulting in a significantly higher disease control rate, longer time to progression, and longer overall survival compared with hepatic arterial infusion chemotherapy using cisplatin. Thus, sorafenib, rather than hepatic arterial infusion chemotherapy, should be considered as the first-line therapy for patients who are refractory to TACE in the future.

Acknowledgments This work was supported in part by Grants-in-Aid for Cancer Research and for the Third-Term Comprehensive 10-Year Strategy for Cancer Control from the Ministry of Health, Labour, and Welfare of Japan.

Conflict of interest The authors declare that they have no conflict of interest.

References

1. Kudo M, Izumi N, Kokudo N, Matsui O, Sakamoto M, Nakashima O, et al. Management of hepatocellular carcinoma in Japan: consensus-based clinical practice guidelines proposed by the Japan Society of Hepatology (JSH) 2010 updated version. Dig Dis. 2011;29:339–64.
2. Bruix J, Sherman M, Practice Guidelines Committee, American Association for the Study of Liver Diseases. Management of hepatocellular carcinoma. Hepatology. 2005;42:1208–36.
3. Cammà C, Schepis F, Orlando A, Albanese M, Shahied L, Trevisani F, et al. Transarterial chemoembolization for unresectable hepatocellular carcinoma: meta-analysis of randomized controlled trials. Radiology. 2002;224:47–54.
4. Llovet JM, Bruix J. Systematic review of randomized trials for unresectable hepatocellular carcinoma: chemoembolization improves survival. Hepatology. 2003;37:429–42.
5. Llovet JM, Bruix J. Molecular targeted therapies in hepatocellular carcinoma. Hepatology. 2008;48:1312–27.
6. Zhu AX. Development of sorafenib and other molecularly targeted agents in hepatocellular carcinoma. Cancer. 2008;112:250–9.
7. Llovet JM, Ricci S, Mazzaferro V, Hilgard P, Gane E, Blanc JF, et al. Sorafenib in advanced hepatocellular carcinoma. N Engl J Med. 2008;359:378–90.

8. Cheng AL, Kang YK, Chen Z, Tsao CJ, Qin S, Kim JS, et al. Efficacy and safety of sorafenib in patients in the Asia-Pacific region with advanced hepatocellular carcinoma: a phase III randomised, double-blind, placebo-controlled trial. Lancet Oncol. 2009;10:25–34.
9. Kudo M, Izumi N, Kokudo N, Matsui O, Sakamoto M, Nakashima O, et al. Management of hepatocellular carcinoma in Japan: consensus-based clinical practice guidelines proposed by the Japan Society of Hepatology (JSH) 2010 updated version. Dig Dis. 2011;29:339–64.
10. Yamashita T, Kaneko S. Treatment strategies for hepatocellular carcinoma in Japan. Hepatol Res. 2013;43:44–50.
11. Bruix J, Raoul JL, Sherman M, Mazzaferro V, Bolondi L, Craxi A, et al. Efficacy and safety of sorafenib in patients with advanced hepatocellular carcinoma: subanalyses of a phase III trial. J Hepatol. 2012;57:821–90.
12. Cheng AL, Guan Z, Chen Z, Tsao CJ, Qin S, Kim JS, et al. Efficacy and safety of sorafenib in patients with advanced hepatocellular carcinoma according to baseline status: subset analyses of the phase III Sorafenib Asia-Pacific trial. Eur J Cancer. 2012;48:1452–65.
13. Iwasa S, Ikeda M, Okusaka T, Ueno H, Morizane C, Nakachi K, et al. Transcatheter arterial infusion chemotherapy with a fine-powder formulation of cisplatin for advanced hepatocellular carcinoma refractory to transcatheter arterial chemoembolization. Jpn J Clin Oncol. 2011;41:770–5.
14. Kirikoshi H, Yoneda M, Mawatari H, Fujita K, Imajo K, Kato S, et al. Is hepatic arterial infusion chemotherapy effective treatment for advanced hepatocellular carcinoma resistant to transarterial chemoembolization? World J Gastroenterol. 2012;18:1933–9.
15. Yoshikawa M, Ono N, Yodono H, Ichida T, Nakamura H. Phase II study of hepatic arterial infusion of a fine-powder formulation of cisplatin for advanced hepatocellular carcinoma. Hepatol Res. 2008;38:474–83.
16. Court WS, Order SE, Siegel JA, Johnson E, DeNittis AS, Principato R, et al. Remission and survival following monthly intraarterial cisplatinum in nonresectable hepatoma. Cancer Invest. 2002;20:613–25.
17. Ueshima K, Kudo M, Takita M, Nagai T, Tatsumi C, Ueda T, et al. Hepatic arterial infusion chemotherapy using low-dose 5-fluorouracil and cisplatin for advanced hepatocellular carcinoma. Oncology. 2010;78(Suppl 1):148–53.
18. Yamasaki T, Kimura T, Kurokawa F, Aoyama K, Ishikawa T, Tajima K, et al. Prognostic factors in patients with advanced hepatocellular carcinoma receiving hepatic arterial infusion chemotherapy. J Gastroenterol. 2005;40:70–8.
19. Obi S, Yoshida H, Toune R, Unuma T, Kanda M, Sato S, et al. Combination therapy of intraarterial 5-fluorouracil and systemic interferon-alpha for advanced hepatocellular carcinoma with portal venous invasion. Cancer. 2006;106:1990–7.
20. Uka K, Aikata H, Takaki S, Miki D, Kawaoka T, Jeong SC, et al. Pretreatment predictor of response, time to progression, and survival to intraarterial 5-fluorouracil/interferon combination therapy in patients with advanced hepatocellular carcinoma. J Gastroenterol. 2007;42:845–53.
21. Monden M, Sakon M, Sakata Y, Ueda Y, Hashimura E, FAIT Research Group. 5-Fluorouracil arterial infusion + interferon therapy for highly advanced hepatocellular carcinoma: a multicenter, randomized, phase II study. Hepatol Res. 2012;42:150–65.
22. Therasse P, Arbuck SG, Eisenhauer EA, Wanders J, Kaplan RS, Rubinstein L, et al. New guidelines to evaluate the response to treatment in solid tumors. European Organization for Research and Treatment of Cancer, National Cancer Institute of the United States, National Cancer Institute of Canada. J Natl Cancer Inst. 2000;92:205–16.

Evaluation of a Near-Infrared–Type Contrast Medium Extravasation Detection System Using a Swine Model

Toshihiro Ishihara, RT,† Tatsushi Kobayashi, MD,* Naoya Ikeno, RT,* Takayuki Hayashi, MD,* Masahiro Sakakibara,‡ Noboru Niki, PhD,† Mitsuo Satake, MD,* and Noriyuki Moriyama, MD, PhD§*

Purpose: To refine the development and evaluate the near-infrared (NIR) extravasation detection system and its ability to detect extravasation during a contrast-enhanced computed tomography (CT) examination.

Materials and Methods: The NIR extravasation detection system projects the NIR light through the surface of the human skin then, using its sensory system, will monitor the changes in the amount of NIR that reflected, which varies based on absorption properties.

Seven female pigs were used to evaluate the contrast media extravasation detection system, using a 20-gauge intravenous catheter, when injected at a rate of 1 mL/s into 4 different locations just under the skin in the thigh section. Using 3-dimensional CT images, we evaluated the extravasations between time and volume, depth and volume, and finally depth and time to detect.

Results: We confirmed that the NIR light, 950-nm wavelength, used by the extravasation detection system is well absorbed by contrast media, making changes easy to detect. The average time to detect an extravasation was 2.05 seconds at a depth of 2.0 mm below the skin with a volume of 1.3 mL, 2.57 seconds at a depth between 2.1 and 5 mm below the skin and a volume of 3.47 mL, 10.5 seconds for depths greater than 5.1 mm and a volume of 11.1 mL. The detection accuracy was significantly deteriorated when the depth exceeded 5.0 mm (Tukey-Kramer, $P < 0.05$)

Conclusions: The extravasation system detection system that is using NIR has a high level of detection sensitivity. The sensitivity enables the system to detect extravasation at depths less than 2 mm with a volume of 1.5 mL and at depths less than 5 mm with a volume of 3.5 mL. The extravasation detection system could be suitable for use during examinations.

Key Words: computed tomography, contrast media, contrast-enhanced CT, extravasation detection

(*J Comput Assist Tomogr* 2014;38: 285–292)

It is common during computerized tomography (CT) examinations for the intravenous injection of contrast media to be performed using an automated power injector (injector). The injector provides the flexibility, consistency, accuracy, and safety precautions necessary to perform the required high speed and pressure injections for CT examinations to obtain clinically acceptable images. With this, however, comes the risk of contrast medium extravasation, which requires careful attention.[1] Wang et al [3,4] reported that, in 69,657 patients who were injected with intravenous contrast medium (CM), 475 patients (0.7%) experienced extravasation, and Chew [3,4] determined that the occurrence of extravasation was 0.45%, applying the Self-Assessment Module Scenario 1 by checking previous reports of extravasation after CM injection.[3,4]

Early symptoms of extravasation include local inflammation, sharp pain, and redness of the skin; however, later and more severe extravasations can result in the destruction of tissue. This comes about because of the difference in osmotic pressure between CM and human blood and body fluids. Although it is considered that the toxicity of nonionic contrast media is generally mild, the osmotic pressure is twice that of body fluids. Therefore, a large volume of extravasated CM may cause critical conditions such as ulcer formation or compartment syndrome.[5–14] In addition, the workflow is disrupted, examination efficiency is decreased, plus the reputation of the facility is negatively affected.[14]

Nelson et al [16,17] report an extravasation detection accessory (EDA) that used strain gauges connected (4 points) in a Wheatstone bridge configuration. This system detects the impedance change under a patch measuring 5 × 8 cm and indicates extravasation when a change limit value is exceeded. It was reported this EDA kept 100% sensitivity for 10-mL extravasations. Bouton et al [18] report an extravasation detection accessory that uses radiofrequency. This system detects the change of conductivity using its 4 radiofrequency transmitter/receiver modules surrounding the puncture point. The average volume of the sensing area is 12.5 mL, and it was reported that the system could detect extravasations from 8 to 10 mL.

Hereinafter we shall focus on the extravasation detection system that uses near-infrared (NIR) light. This system uses the absorption characteristics of NIR light by the CM, monitoring the changes of absorption of the scattered NIR light just under the skin.[18–20]

For our evaluation, 7 swine models were used to simulate the extravasation of contrast media inside the thigh skin and evaluate the duration, depth, and volume of extravasation to demonstrate the effectiveness of the system.

MATERIALS AND METHODS

Contrast Media Extravasation Detection System

Overview of the System

The contrast media extravasation detection system consists of 3 parts: a sensor part that includes an alarm box to indicate when contrast media is extravasating, a receiver, and a computer (Windows XP; Dell) that is used to analyze the signal. The configuration is shown in Figure 1. The sensor part detects the intensity changes of the scattered light illuminated into the skin compared with the base intensity that is measured before the

From the *Department of Radiology, National Cancer Center Hospital East; †Graduate School of Functional Systems Engineering, The University of Tokushima; ‡Nemoto Kyorindo Co., Ltd.; and §Research Center for Cancer Prevention and Screening, National Cancer Center, Japan.

Received for publication May 30, 2013; accepted September 9, 2013.

Reprints: Toshihiro Ishihara, RT, Department of Radiology, National Hospital Organization Saitama National Hospital, 2-1, Suwa, Wakho city, Saitama, 351-0102, Japan (e-mail: tishihar@hotmail.com; tishihar@wakho.hosp.go.jp).

T. Ishihara is now with the National Hospital Organization Saitama National Hospital. N. Ikeno is now with the National Hospital Organization Disaster Medical Center. M. Sakakibara is now with Mono Well-being Co., Ltd.

This work was supported in part by the Grant-in-Aid for Cancer Research (21S-1) from the Ministry of Health, Labour and Welfare.

The summary of this study was announced in the 2010 annual meeting of European Society of Radiology.

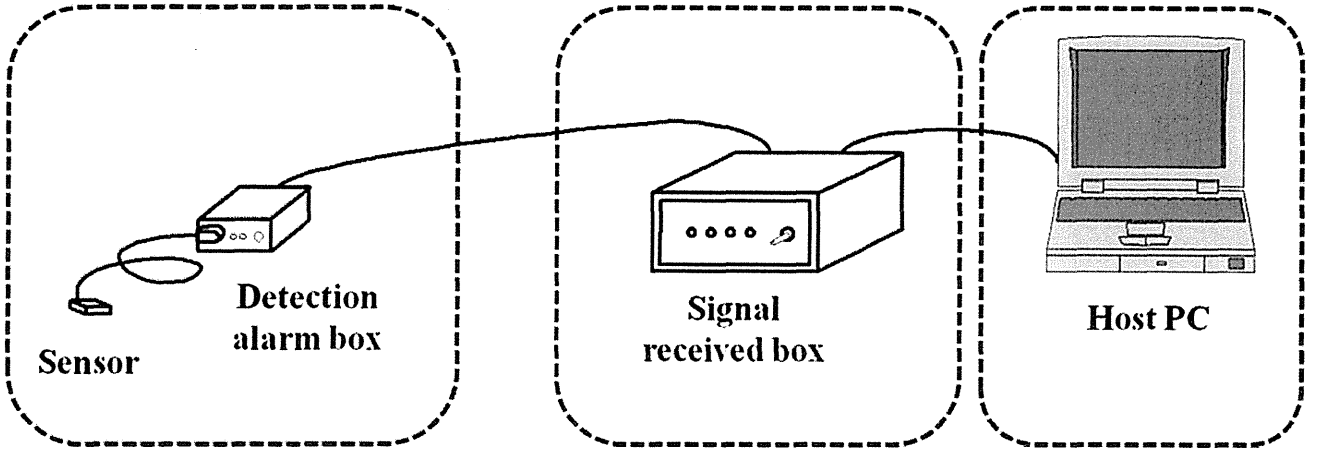

FIGURE 1. Extravasation detection system block diagram. The system is composed of three parts: the calculation unit, the box for receiving (including the box leak detector contrast medium), the leak-detecting sensor signal, the signal sensing, and the signal received. Device used to perform a spectral analysis of the reflected light.

injection. These intensity changes are converted and measured as a change in voltage. When an extravasation occurs, the voltage signal from the sensor part will decrease. Once the voltage decreases below the lower limit, the system will signal an alarm. The computer displays the voltage fluctuation as a trend graph.

Contrast Media Extravasation Detection Sensor

Determination of Light-Absorption Characteristics of Human Skin

Using the diffuse reflectance method, the light-absorption characteristics of human skin around the median cubital vein were measured. For the light source, an incandescent lamp (GA-30H; ELPA) was used because it has a wide optical spectrum. A spectrometer (InGaAs NIR Spectrometer EPP-2000; StellartNet) was used to measure the reflected light. The measuring device is shown in Figure 2. To obtain a baseline for the total reflected light intensity, the incandescent lamp was directed to a white board maintained at a distance of 50 mm and the reflected light was measured. The lamp was then shaded with a black board, and another measurement was made to determine the reflected amount with 100% absorption. Finally, we directed the lamp toward human skin and measured the scattered light. Compared with the total reflected light possible, we confirmed that the option spectrum was 600 to 1000 nm (Fig. 3).

Determination of Absorption Characteristics of Water and Contrast Media

To determine the absorption characteristics of water and contrast media, we used the transmit method. Again, the incandescent lamp was used for the light source and the spectrometer was used to measure the light. Tools were used to prevent the ambient light from affecting our measurements of characteristics of water and contrast media. The measurement system is shown in Figure 4. To determine the absorption characteristics, the lamp was placed on one side of the spectrometer the other side of the

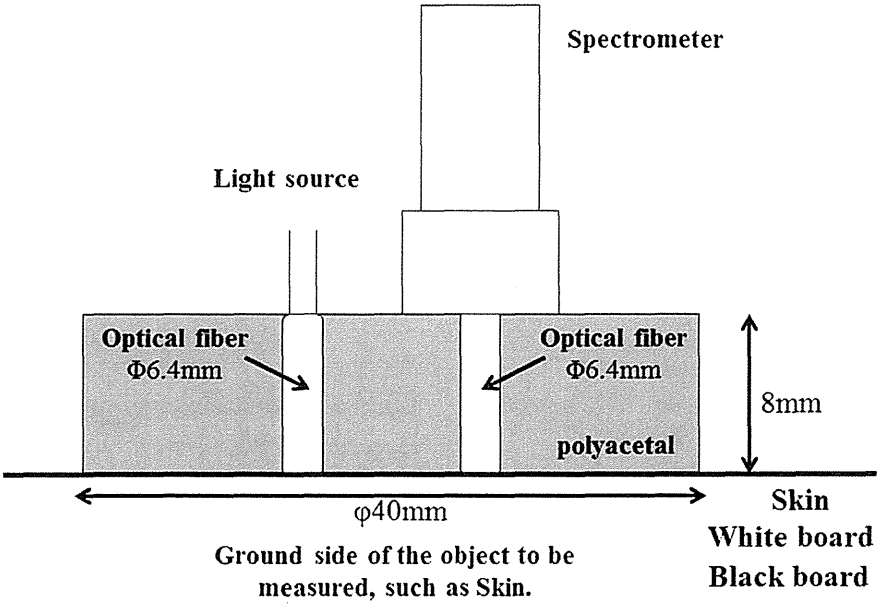

FIGURE 2. Diagram. Detector to measure the light absorption characteristics. Measuring the light absorption characteristics of the reflected light.

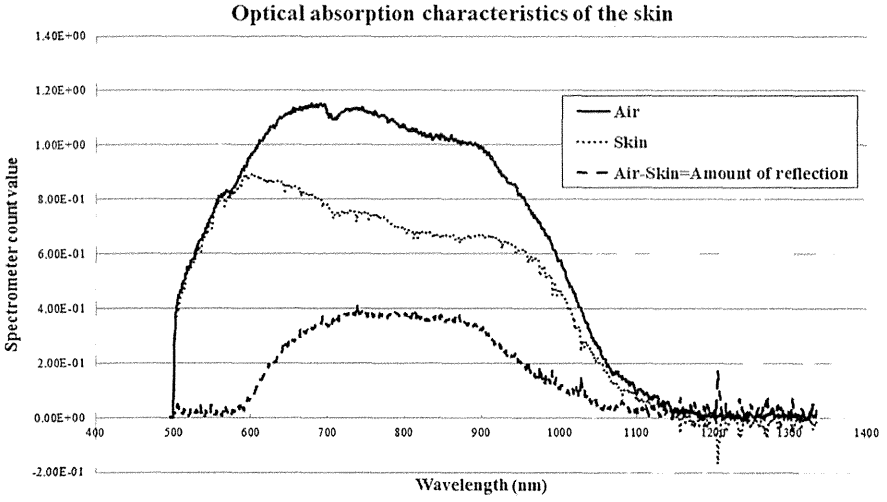

FIGURE 3. The spectrum of light reflected was measured at 600 to approximately 1000 nm for human skin compared with total reflection of light in the air.

water and contrast media. The absorption spectrum band was specifically identified at 950 nm wavelength (Fig. 5). It was determined from these results that a wavelength of 950 nm is ideal to permeate and scatter in the human skin and provide adequate changes based on the absorption by water and contrast media.

Configuration of Contrast Media Extravasation Detection Sensor

For the contrast media extravasation detection sensor, NIR LED (AN1111R; Stanley) having a peak wave length of 950 nm was used for light source and NIR phototransistor (PS1101WA; Stanley) was used for the detector.

The configuration is shown in Figure 6.

The contrast media extravasation detection sensor emits light at a wavelength of 950 nm, NIR, into the human skin, then a measurement of the intensity of reflected light intensity is made using the phototransistor. Comparing the reflected light intensity before injection with the intensity of reflected light during the contrast media injection makes the detection of extravasation possible. If a sufficient amount is absorbed, then an extravasation is suspected and reported.

Determination of Measurement Point of Swine Model

The National Cancer Research Center Animal Study ethics committee and ethics committee of the institute approved this study using animals for data collection of human subjects.

A location with similar hardness and absorption characteristics with the upper median cubital vein of humans for intravascular contrast enhancement CT examination was chosen in the swine model (Specific Pathogen–Free).

The skin hardness was measured on the upper median cubital vein with 6 volunteers (2 women, 4 men; age range, 28–43 years; mean age, 34 years; body mass index range, 17.8–27.6 kg/m^2; mean body mass index, 22.8 kg/m^2) and the 5 points were the abdomen and outer thigh and inner thigh of both legs of 2 swine models (body weight, 30.2 and 31.5 kg).

Skin hardness was measured with a durometer (ASTM D 2240, GS754H, TypeOO Durometer; Teclock Ltd., Okaya, Japan). Three measurements were made then averaged to determine the skin hardness. Note that the hardness measurement is a relative physical amount and has no units of measure. In addition, the absorption characteristics were also measured in the same location, again 3 times then averaged, using the measuring equipment shown in Figure 2 to determine the absorption characteristics.

Evaluation With Swine Model

Simulate an extravasation on 7 swine models and evaluate the performance of contrast media extravasation detection system.

1. The puncture area was chosen based on having similar skin hardness and absorption characteristics as the upper median cubital vein of our human skin measurements. A 20-gauge intravenous catheter (Terumo) was inserted by a physician, and the depth of insertion was adjusted to 1.0 to 10.0 mm. The extravasation detection sensor was placed such that the center of the sensor was positioned 5 mm from the catheter tip and light source. Refer to Figure 7.
2. To set the baseline, the light intensity level before the injector was measure and recorded via the computer. A contrast injection via a power injector (Dual Shot; Nemoto Kyorindo, Tokyo, Japan) was performed at a rate of 1.0 mL/s. The light intensity was observed and compared with that of the baseline during the injection. The contrast media was Iohexal 300 that was diluted 3 times with saline to decrease the influence of artifact.
3. The physician stopped the injection when the light intensity level exceeded the limit. After the injection was stopped, the detection duration and the volume of extravasation were determined.
4. After the extravasation was detected, an image via CT scanner (Aquilion 4; Toshiba Medical Systems, Ootawara, Japan) of the injected area along with the sensor still applied was completed (Fig. 8).

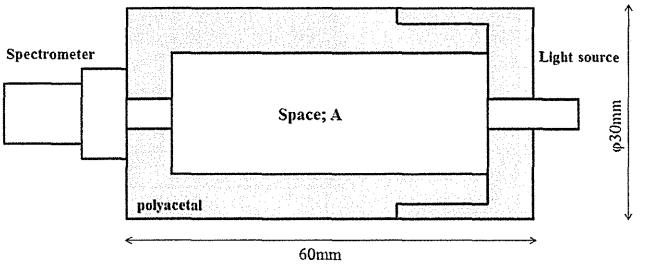

FIGURE 4. Measuring devices for light absorption characteristics of the contrast medium, water, and air. Used to eliminate the effect of ambient light shielding.

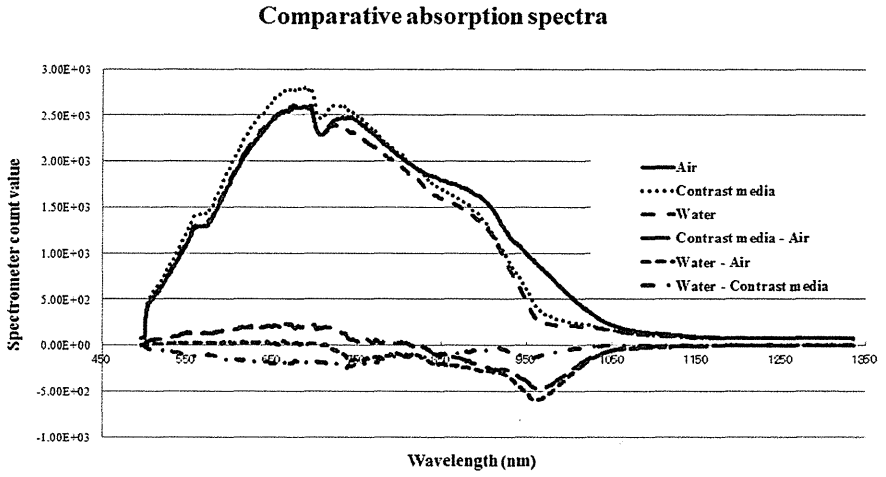

FIGURE 5. Absorption spectrum of the contrast medium with water, which absorbs light at a wavelength of 950 nm specifically, as compared with that passed through air.

Imaging condition of CT was 120 kV, 400 mA, 0.5 sec/rotation speed; low slice thickness, 1.0 mm; pitch factor, 0.875; image slice thickness, 1.0 mm.

5. The depth of the extravasated contrast media was measured using the CT images. Using the profile curve of the CT value, we obtained the distance between the sensor surface on the skin and edge of contrast media. The depth measurement from the skin surface was defined using the full width at 10 maximum (FWTM) of profile curve.

RESULTS

Determination of Measuring Point and the Result of the Swine Model

Skin hardness of human and swine model was measured by the durometer, as shown in Tables 1, 2. The average of skin hardness around the cubital vein was 45.4, and its SD was 0.82. The inside thigh skin of 2 swine models, average was 45.4 and SD was 0.28. Similar skin hardness between inside thigh skin of swine model and cubital vein of human is shown.

Absorption characteristics of cubital vein and inside thigh skin of swine model are shown in Figure 9. Each absorption characteristics shown is in the range of 600 to approximatey 1000 nm, demonstrating similar characteristics.

Result of Swine Model Examination

The relation between the detection duration, depth of extravasation, and extravasated volume for total 28 points of the 7 swine models and 4 points of inside thigh skin are shown in Figure 10A, B.

Figure 10A shows the difference of the extravasated volume compared with the detection time.

A minimum extravasated volume (0.9 mL) could be detected in 2.0 seconds. A shorter detection duration shows a lower extravasated volume. Detection duration and leakage volume were classified into 3 groups (detection duration: group I, 0–3 seconds; group II, 3.1–6 seconds; group III, 6.1–16 seconds). Extravasated volume was 0.9 mL in a detection duration of 2.0 seconds and the average was 3.7 mL in group I; average volume was 8.8 mL in an average detection duration of 5.2 seconds in group II; in group III, the maximum volume was 13.0 mL in 15.0 seconds and the average volume was 13.0 mL in an average duration 14.0 seconds. Correlation between detecting duration and volume were $R^2 = 0.85$, and a positive correlation is shown. When applying the statistical test (Tukey-Kramer), no significance difference was shown between groups I and II; however, comparing group III with groups I and II showed a significant difference because $P < 0.05$. It is also shown that a longer detection time causes an increase in extravasated volume.

Figure 10B shows the difference between the extravasated volumes compared with the depth of extravasation. A minimum extravasated volume (0.9 mL) could be detected in extravastion depths of 0.98 mm. A deeper extravasation leads to an increase in extravasation volume. The depth of extravasation and leakage volume were classified into 3 groups (depth: group I, 0–2.0 mm; group II, 2.1–4.2 mm; and group III, 4.3–10.2 mm); extravasated volume was 0.9 mL in a depth of 0.98 mm and the average was 1.1 mL in group I, average volume was 3.1 mL in group II and the average volume was 6.9 mL. Correlation between detecting duration and volume was $R^2 = 0.85$, and a positive correlation is

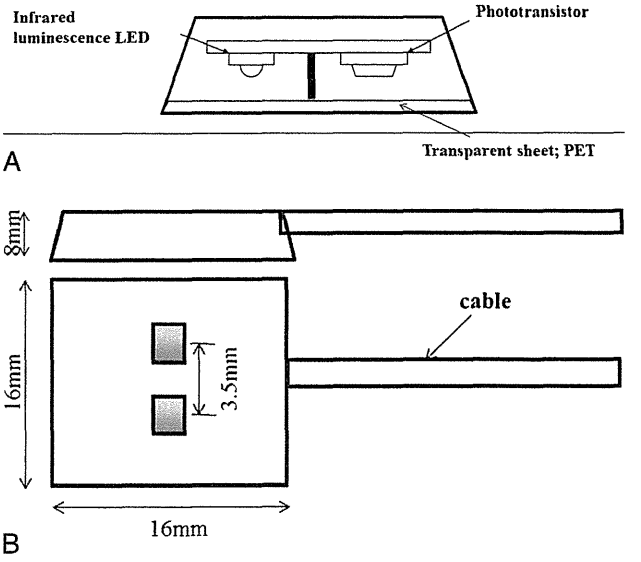

FIGURE 6. Diagram sensor head. Using a phototransistor (Stanley AN1111R), you place the sensor structure (PS1101WA Stanley) LED with infrared emission peak wavelength of 950 nm onto the light source.

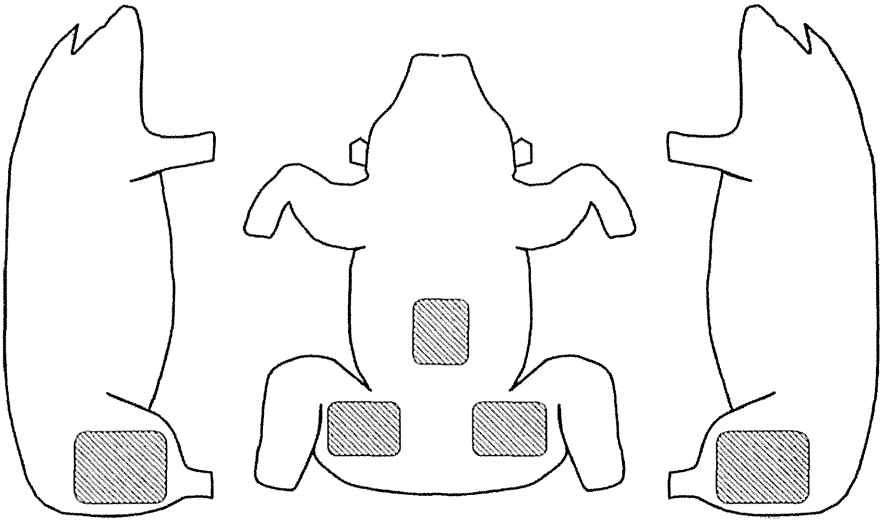

FIGURE 7. Summary installing the sensor in the swine model.

shown. When applying the statistical test (Tukey- Kramer), no significance difference is shown in groups I and II; however, comparing group III with groups I and II shows a significant difference because $P < 0.05$. It is also shown that the delay of detection duration increases with extravasated volume.

The leak positions were classified into 6 groups in accordance with their depths (group I, within 1 mm; group II, 1.1–2.0 mm; group III, 2.1–3.0 mm; group IV, 3.1–4.0 mm; group V, 4.1–5.0 mm; and group VI, 5.1 mm or more), and the average leak volume and average detection time in each leak depth group were compared.

In the case of group II, it was possible to detect within a detection time of 2.1 seconds or less with a leak volume of 1.32 mL or less. In the case of group III, it was possible to detect under within 2.7 seconds or less with a leak volume of 2.7 mL or less. However, in the case of group III, the detection time was 10.5 seconds and the leak volume was 11.1 mL, which showed a remarkable increase. In the multiple simultaneous hypotheses testing (Tukey-Kramer), no significant differences were observed in the leak volumes in I to IV ($*P < 0.05$), but a significant difference was observed in I to VI ($*P < 0.05$), II to VI ($*P < 0.05$), III to VI ($*P < 0.05$), IV to VI ($*P < 0.05$), V to VI ($*P < 0.05$). Regarding the detecting duration, no significant differences were observed in I to IV, significant differences were observed in I to VI ($*P < 0.05$), II to VI ($*P < 0.05$), III to VI ($*P < 0.05$), IV to VI ($*P < 0.05$), and V to VI ($*P < 0.05$) (Fig. 11). As for the contrast medium extravasation detection system, no false-positives or false-negatives were identified. From the above results, extravasation volume could be detected in 1.3 mL in 2.0 mm, and 3.5 mL in 5.0 mm could be detected, and high detection sensitivity was shown.

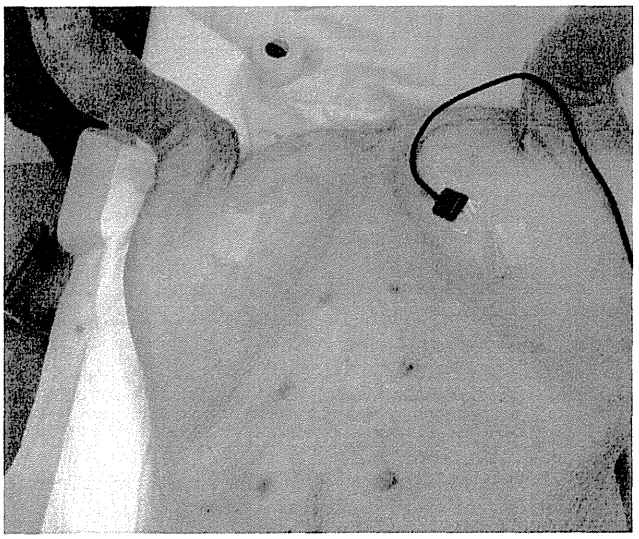

FIGURE 8. CT image showing extravasation in the swine model. The contrast medium accumulated in the right inner thigh.

DISCUSSION

We developed the contrast extravasation detection system, discussed the detection accuracy, and examined the detection performance during an intravenous contrast-enhanced CT examination using a swine model.

The detection accuracy of the contrast detection system that used NIR is high, and an extravasated volume of 1.3 mL could be detected at 2.0 mm depth, and 3.5 mL could be detected within the depth of 5.0 mm. The correlation between the leakage volume and the leakage point showed that deeper extravasations result in increases in the extravasation volume. As for detection accuracy of the contrast medium extravasion detection system, it was confirmed that a deeper contrast medium

TABLE 1. Cubital Vein Measurements in 6 Volunteers

Human			
Volunteer	Sample No.	Hardness	Part
A	1	45.1	Elbow
B	4	46.4	Elbow
C	7	44.8	Elbow
D	10	46	Elbow
E	13	44.2	Elbow
F	16	45.7	Elbow
Average: Elbow		45.36667	
SD: Elbow		0.816497	

The average hardness of the skin was 45.4 ± 0.82.

TABLE 2. Search Results for 5 Hardness Measurements of the Human Body at the Same Level as the Upper Cubital Vein Swine Model of 2 Animals

Swine Model			
Pig	Sample No.	Hardness	Part
x	1	45.2	Rt. thigh on inside
	2	46.4	Lt. thigh on inside
	3	69.3	Rt. thigh on outside
	4	60.2	Lt. thigh on outside
	5	50.1	Abdomen
y	6	44.8	Rt. thigh on inside
	7	45.3	Lt. thigh on inside
	8	70.5	Rt. thigh on outside
	9	63.4	Lt. thigh on outside
	10	52.7	Abdomen
Average: Thigh on inside		45.425	
SD: Thigh on inside		0.2828427	
Average: Thigh on outside		63.4	
SD: Thigh on outside		4.8802322	
Average: Abdomen		51.4	
SD: Abdomen		1.8384776	

The skin of the inner thigh hardness was 45.4 ± 0.28.

leak position resulted in a longer detection time. There was a correlation between the leakage depth and the leakage volume.

Especially, for example, a leak depth of 5.1 mm or more resulted in a detection time of 10.5 seconds or more. Comparing this with a leakage depth of 5.0 mm or less, the leakage volume significantly increased. It was suggested, however, that there

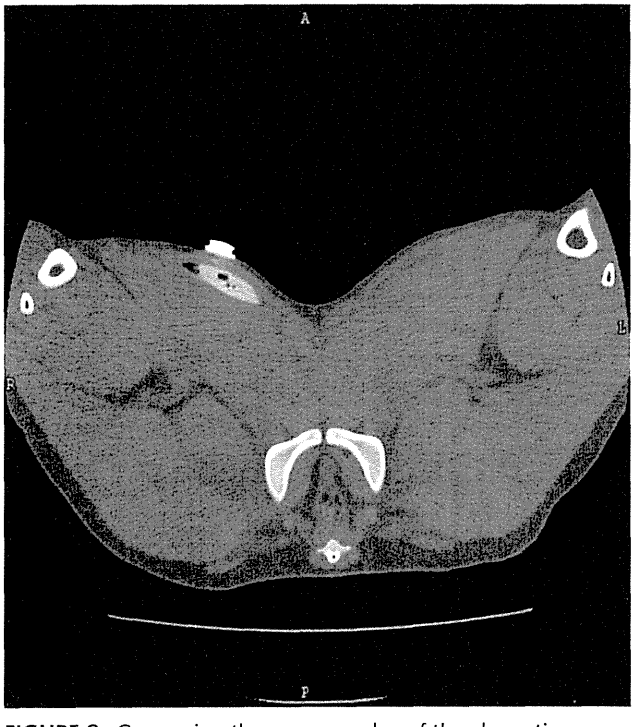

FIGURE 9. Comparing the average value of the absorption characteristics of the pig and the human body. Light absorption characteristics are equivalent.

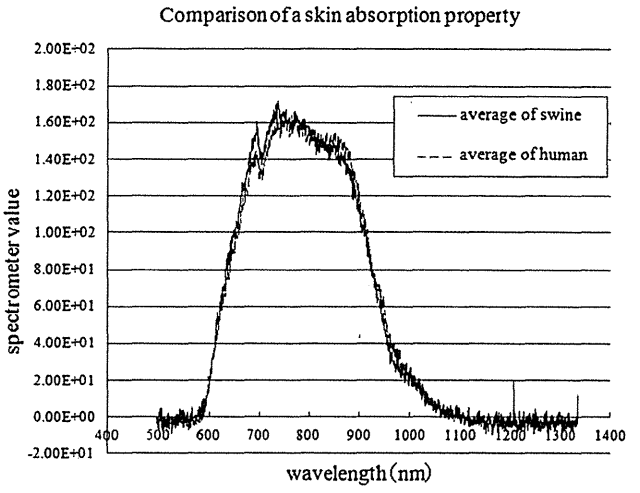

FIGURE 10. A, Relationship between the amount of time and leakage detection. Leakage increases with the increase of leakage detection time. B, Relationship between the amount of leakage and leakage position. Leakage increases with increasing depth of the leak position.

may be several opportunities to improve the device wherein detecting deeper extravasations more accurately would become possible. There is an adequate correlation to the natural logarithm to the depth, detection level, and the transmission loss of light that could enable variations in the operating algorithms to be considered. It was also shown that the rise time of the injection until the flow rate setting is achieved is directly related to the mechanical accuracy of the injector; therefore, mechanical improvements are possible. Finally, testing with human subjects

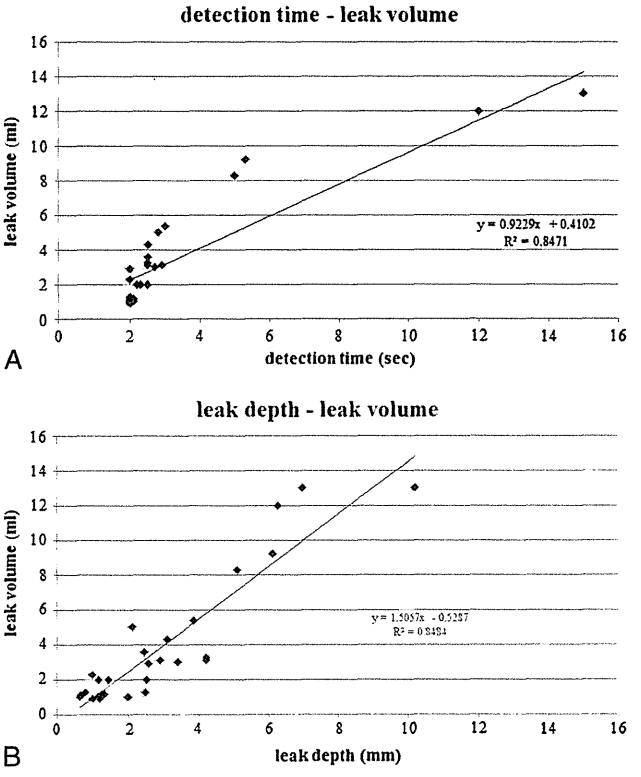

FIGURE 11. Comparison of the amount of leakage and the detection time.

would help in determining the detection influences that were caused by the puncture point resistance by using the swine model. Furthermore, the delay time from when the sensor detects extravasation until the injection stops is influenced by the systems configuration and human factors. From this delay time, the injection volume can be calculated; therefore, improving the system response time can reduce the injected volume before the injection stops.

Based on the results, the contrast medium extravasation detection system could prevent serious diseases such ulcer formation and compartment syndrome by detecting extravasations at their early stage if used at clinical sites. The contrast medium extravasation detection system, if used in the clinical setting, could decrease the probability of occurrence of compartment syndrome with its ability to detect extravasation early and minimize the extravasated amount of contrast. Sistrom et al [22] classified the amount of extravasation into 3 groups (minor, <10 mL; moderate, 10–49 mL; major, ≥50 mL) plus related each group to the damage.

Clinically, it is generally accepted that the contrast medium leak volume, from which the subject feels pain, is about 5.0 to 10 mL. Our newly developed contrast medium extravasation detection system can detect extravasation of about 1 mL and allows stopping injection of the contrast medium before the subject feels pain. Moreover, when the contrast medium extravasation detection system is interfaced with the injector and contrast medium extravasation is detected, it is possible to stop the contrast medium injection automatically. Therefore, interconnecting the two systems is highly recommended, if not indispensable.

It should be noted though, with the sensor tip set close to the tip of the catheter needle, there might be a case that the contrast medium extravasation occurs in the area where the sensor cannot detect it. Therefore, it is necessary to properly install the sensor, noting the effective range of the sensor.

In this study, the injection flow rate of the contrast medium was 1.0 mL/s, but at present, many facilities perform CT examinations at higher flow rates (3.0–5.0 mL/s) that heightens the risk of extravasation.[23–25] However, Jacobs et al [26] propose that there is no correlation to the contrast medium injection flow rate and frequency of extravasation. As for the relation between injection flow rate and contrast medium extravasation, further investigation is needed, taking into account the patients' age and sex, a punctured blood vessel, the catheter needle size, and so on. However, if the flow rate of contrast medium increases, the leak volume per unit time increases. Therefore, the relation between the contrast medium extravasation detection system detection speed and the contrast medium injection flow rate needs further consideration. This study was also limited to only Japanese patients, and although good results were obtained, additional factors, for example, the skin thickness, skin color, hardness, and thickness of the hypodermis should be considered for further study.

There are several advantages that can be considered by using the contrast medium extravasation detection system in everyday CT examinations. For example, incommunicable patients such as small children including infants, the elderly, sedated, or unconscious patients, wherein the injection could be stopped automatically for even small volumes of extravasation. Early detection could also prevent the critical side effects before they occur.

Furthermore, by preventing ulcer formation and compartment syndrome, the system contributes to mitigate the mental burden and minimizes the medical treatment time on the side of our medical staff as well as patients when extravasations occur.

Paice [15] reported in *Imaging Economics* ("extravasation," an analysis that the economical effect due to the extravasation with considering the criticality of the damage and the reparation for injury) the economic impact of an extravasation. It is necessary to prevent the economical loss even with a low probability of occurrence, according to Paice. Also, the occurrence of an extravasation, because of its interruption of the CT examination, decreases the CT department efficiency, along with an adverse impact on the reputation of the hospital.

Often, monitoring with x-rays is performed shortly after the start of a contrast medium injection (eg, bolus tracking method, etc.), medical staff must evacuate from the examination room to avoid being exposed to radiation. However, before leaving the room, they must ensure that the complete dose was injected to the patient.

Therefore, to prevent the risk of contrast medium extravasation, operators take the risk of being exposed to radiation. If, however, the contrast medium extravasation detection system is used, it is possible to avoid unnecessary radiation.[26–30] Sometimes, contrast medium extravasation occurs after the medical staff has confirmed proper puncture, catheter insertion, and left the imaging room. In this situation, it is difficult to decide whether to stop the contrast medium injection or to continue. However, if extravasation is detected with the contrast medium extravasation detection system, the medical staff can be assured that extravasation really occurred, and the injection can be stopped automatically without the medical staff being exposed to radiation.

Developing a system to detect contrast medium extravasation during an intravenous CT imaging examination plays an important role in securing higher levels of safety and reliance on the examinations. Moreover, if the injector and contrast medium extravasation detection system are manufactured by the same manufacturer as the injector, it makes it possible to interconnect systems, providing a solution for minimizing extravasations. This detection system was developed by joint research with the injector manufacturer. Therefore, our detection system provides a high level of safety to the clinical sites.

CONCLUSIONS

The detection accuracy was verified with similar absorption characteristics of human cubital vein and the swine model. The contrast medium extravasation detection system using NIR to detect contrast medium extravasation occurrence could detect within 2 seconds at depths of 2.0 mm or less and a leak volume of 11.1 mL in 10.5 seconds at the maximum depth of 10.2 mm under the skin. Early detection of extravasation at volumes of 3.5 mL at the depth of 5 mm could decrease the risk of serious extravasation.

REFERENCES

1. Schaverien MV, Evison D, McCulley SJ. Management of large volume CT contrast medium extravasation injury: technical refinement and literature review. *J Plast Reconstr Aesthet Surg*. 2008;61:562–565.
2. Wang CL, Cohan RH, Ellis JH, et al. Frequency, management, and outcome of extravasation of nonionic iodinated contrast medium in 69,657 intravenous injections. *Radiology*. 2007;243:80–87.
3. Chew FS. Extravasation of iodinated contrast medium during CT: self-assessment module. *AJR Am J Radiol*. 2010;195:S80–S85.
4. Antebi A, Herscovici D Jr. Acute compartment syndrome of the upper arm: a report of 2 cases. *Am J Orthop*. 2005;34:498–500.
5. Dhawan V, Borschel GH, Brown DL. Acute exertional compartment syndrome of the forearm. *J Trauma*. 2008;64:1635–1637.
6. Upton J, Mulliken JB, Murray JE. Major intravenous extravsation injuries. *Am J Surg*. 1979;137:497–506.